Long-term mission of the spacecraft with a degrading solar sail into the asteroid belt

Bakhyt N. ALIPOVA[a,**], Olga L. STARINOVA[b], Miroslav A. Rozhkov[b]

[a] *Department of Aerospace and Mechanical Engineering, University of Kentucky, Lexington KY, USA, International Information Technology University, Almaty, Kazakhstan*

[b] *Flight Dynamics and Control Theory Department, Samara national Research University, Samara, Russia*

Abstract

The Mars-Jupiter asteroid belt remains one of the least explored regions of the solar system. The use of the Solar Sail Spacecraft (SSSC) will enable a long-term mission into the asteroid belt. We propose the following ballistic scheme for the mission: (1) at the first stage, the upper stage of the launch vehicle takes the SSSC out of the Earth's action sphere and imparts to it the necessary hyperbolic excess velocity; (2) the SSSC makes an Earth-Earth flight, ending with a gravitational manoeuvre in the Earth's action sphere and entering a trajectory with an aphelion of 3.6 AU and zero inclination; then due to the use of light pressure, a circular orbit is formed with a semi-major axis of 2.9 AU; (3) at the last long stage of research, the SSSC is oriented perpendicular to the direction of the light flux and moves along a twisting spiral. At the same time, the spacecraft will fly over and study many objects of the asteroid belt. In this paper, a complete ballistic calculation of this mission is carried out for a degrading solar sail with a non-ideally reflective surface [1]. In addition, during the mission, mathematical models of the SSSC movement and degradation of its surface will be refined.

Keywords: Solar Sail Spacecraft (SSSC), asteroid belt, gravitational manoeuvre, Earth, degrading solar sail

1. Description of the ballistic scheme of the mission and the design parameters of the spacecraft

1.1. Ballistic scheme of the mission

We propose to carry out a long-functioning spacecraft mission with a solar sail to the main asteroid belt according to the following ballistic scheme. A spacecraft with a folded sail is brought out of the Earth's sphere of action onto a heliocentric flight trajectory that provides the specified parameters of a gravitational manoeuvre near the Earth due to the propulsion system of the upper stage. A year later, after performing a gravitational manoeuvre in the Earth's gravity field, the spacecraft fairing is reset and the solar sail opens. Further heliocentric movement is carried out due to light pressure and the spacecraft enters orbit, most of the time lying in the asteroid belt. The solar sail assumes a position perpendicular to the light stream, and further trajectory changes occur only due to the degradation of the sail surface, long-term studies of the asteroid belt are carried out.

1.2. Prototype spacecraft and sails

As a prototype, the solar sail of the SPACECRAFT project is used to deliver soil samples from the surface of Mercury to Earth [2]. The main design parameters of the spacecraft under consideration are given in Table 1, and its mass characteristics in Table 2. According to the calculations of the authors [2], a frame-type solar sail delivered by a Japanese H-2A launch vehicle with an excess of speed to reach a heliocentric trajectory will be able to give a payload weighing 1905 kg an acceleration of 0.25 * 10-3 m/s^2. Fig. 1 shows the placement of this spacecraft under the fairing of the H-IIA launch vehicle.

Table 1. Design parameters of the spacecraft [4]

Weight of the device, kg	Payload weight, kg	The mass of the solar sail, kg	Sail shape, m	Acceleration, m/s^2	Sail thickness,mkm	
					Polyimide CP1	Aluminum
2353	1905	448	275x275	$0.25 \cdot 10^{-3}$	2	0.1

* Corresponding author, alipova.bakhyt@gmail.com

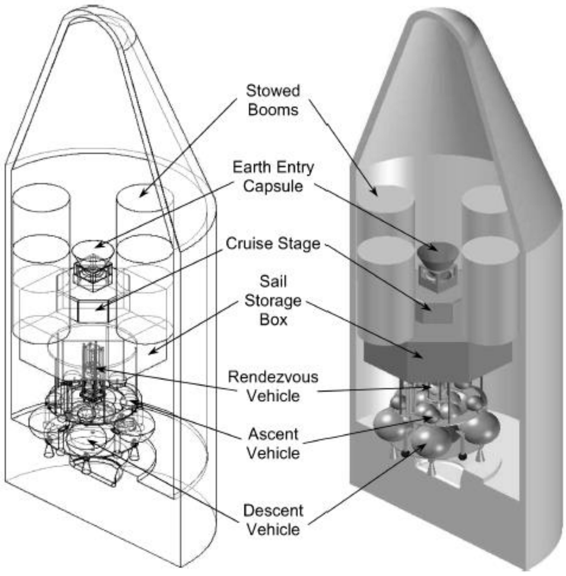

Fig. 1. Placement of a spacecraft with a solar sail delivering soil from the surface of Mercury under the fairing of the H-IIA launch vehicle [2].

Table 2. Mass characteristics of the solar sail for the delivery of Mercury soil

Element Description	Weight, kg
Payload weight of the sail	1905
The bearing film of the CP1 sail is 2 mkm	216
Aluminum reflective coating with a thickness of 0.1 mkm	41
Binding coating	26
Frame beams sails	54
Mechanical deployment and management systems	111
Total mass of solar sail assembly	448
Initial mass of the spacecraft	2353

The dimensions of the solar sail of such a space transport system is 275 by 275 m, which forms a sail area of 75625 m^2 and provides a characteristic acceleration of 0.25 mm/s^2during the flight from Earth to Mercury and 0.78 mm/s^2 on the way back, since the descent compartment and docking mechanisms are discarded at Mercury. The energy characteristics of the Japanese H-IIA 202-4S launch vehicle, with the reference of which the device was designed, make it possible to put up to 2,600 kg of payload into a parabolic orbit out of the Earth's sphere of action (11.2 km/s). This project demonstrates the possibilities of creating space transport systems with a solar sail capable of transporting a payload of about 2 tons between planets.

We chose a lighter spacecraft weighing 500 kg for our calculations, since it is intended for research, not for payload delivery. In this case, the sail area can also be reduced to 16070 m^2. The remaining parameters of the spacecraft under consideration are presented in Table 3.

Table 3. Parameters of the selected spacecraft

Design parameters of the device		Meaning
Initial mass of the spacecraft, kg		500
Sail area, m2		16070
Reflection Coefficient (Al)		0,777
Specular Reflection Factor (Al)		0,900
Secondary radiation coefficient	Al	0,540
	Cr	0,540
Non-Lambert coefficient	Al	0,790
	Cr	0,550

2. The mathematical model used for the motion of a spacecraft with a solar sail

2.1. Mathematical model of motion

The following assumptions are used to describe the motion of the spacecraft:

- the motion of the spacecraft in the plane of the ecliptic is considered, the orbits of the planets are considered circular;

gravitational or other disturbances from any celestial objects are not taken into account;

- the intensity of the Sun's radiation varies inversely proportional to the square of the distance and does not change with time (does not depend on solar activity).

The system of differential equations of motion is described in a flat polar coordinate system in a dimensionless form:

$$\frac{dr}{dt} = V_r, \qquad \frac{dV_r}{dt} = a_r(r, \lambda_1, t) - \frac{1}{r^2} + \frac{V_u^2}{r},$$
$$\frac{du}{dt} = \frac{V_u}{r}, \qquad \frac{dV_u}{dt} = a_u(r, \lambda_1, t) - \frac{V_r V_u}{r} \tag{1}$$

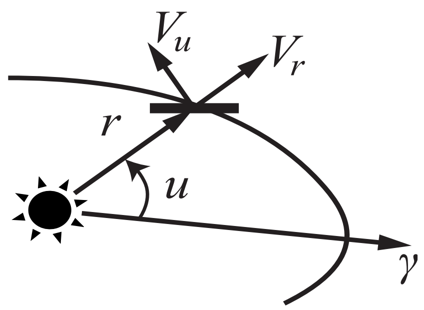

Fig. 2. Polar plane heliocentric coordinate system

Here r, u are the coordinates of the apparatus (radius vector and latitude argument), V_r, V_u are the radial and transversal components of the velocity vector, a_r, a_u are the projections of acceleration generated by the solar sail, the magnitude of which depends on the distance to the Sun r and the angle of the sail λ_1. The coordinates and directions of the vectors are shown in Fig. 2.

In the system of Eq. 1, the phase coordinates of the spacecraft are related to the average radius of the Earth's orbit around the Sun, the average circular velocity and the centripetal acceleration of the Earth. The latitude argument is counted counterclockwise from the axis of the polar coordinate system, which begins at the center of mass of the Sun and is directed towards the point of the vernal equinox.

The boundary conditions correspond to the achievement of the spacecraft target orbit and have the form

$$t = T, \qquad r = r_t, \quad V_r = V_{r_t}, \qquad V_u = V_{u_t}, \tag{2}$$

where T is the duration of the flight, r_t, V_{r_t}, V_{u_t} are the heliocentric radius and velocity components in the target orbit, which depend on the angle of the true anomaly at the final moment of time.

2.2. Acceleration from an imperfectly reflective degrading solar sail

The acceleration of a spacecraft with a flat imperfectly reflecting sail from the light pressure is the sum of two components: directed along the normal to the surface of the sail ($a_\perp$) and parallel to the surface of the sail in a plane passing through the radius vector ($a_{||}$) [3].

$$a_\perp = \frac{S_r}{cm} S \cdot \cos\theta \cdot (a_1 \cos\theta + a_2) \tag{3}$$

$$a_{||} = \frac{S_r}{cm} S \cdot \cos\theta \cdot a_3 \sin\theta \tag{4}$$

$$a_1 = 1 + \varsigma\rho,$$

$$a_2 = B_f(1-\varsigma)\rho + (1-\rho)\frac{\varepsilon_f B_f - \varepsilon_b B_b}{\varepsilon_f + \varepsilon_b},$$

$$a_3 = 1 - \varsigma\rho, \tag{5}$$

where S_r - is the power of the solar electromagnetic wave incident on a unit surface of a sail located at a heliocentric distance r; c - the speed of light; m - the mass of the spacecraft; S - surface area of the sail; θ - the angle between the direction to the Sun and the normal to the surface of the sail (installation angle); ρ - reflection coefficient; ς - the mirror reflection factor of the sail surface; ε_f, ε_b - the radiation coefficients of the front and rear surfaces of the sail; B_f, B_b - are non-Lambert coefficients of the front and rear surfaces of the sail, which describe the angular distribution of emitted and diffusely reflected photons. For the front, reflective surface of a solar sail, well-reflecting aluminium or beryllium are usually chosen. For the rear surface, on the contrary, a well-radiating chrome is chosen (to maintain a moderate sail temperature). The power of the solar electromagnetic wave varies inversely-proportional to the square of the heliocentric distance:

$$S_r = S_0\left(\frac{r_0}{r}\right)^2, \tag{6}$$

where $S_0 = 1{,}36 \cdot 10^3$Вт/м^2 – solar constant (the intensity of the Sun's radiation in the Earth's orbit): $r_0 = 1$ a.e.$= 1{,}496 \cdot 10^8$ km - is the average distance from the Earth to the Sun.

An imperfect reflection from the surface of the sail leads to several negative effects.

Firstly, it is a decrease in the magnitude of acceleration from the forces of light pressure

$$a = \frac{S_r}{cm} S \cos\theta \sqrt{1 + 2\varsigma\rho\cos 2\theta + (\varsigma\rho)^2 + 2a_2(1+\varsigma\rho)\cos\theta + a_2{}^2} \tag{7}$$

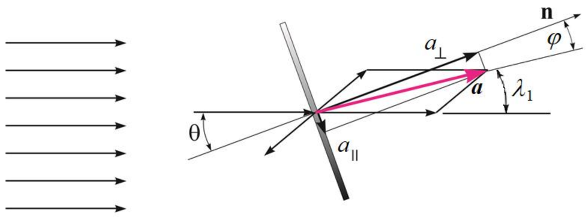

Fig. 3. Magnitude and direction of acceleration

and the deviation of the thrust created by the sail from the direction of the normal to the surface of the sail by an angle φ at Fig. 3.

$$tg\varphi = \frac{a_{||}}{a_\perp} = \frac{a_3 \sin\theta}{a_1\cos\theta + a_2} = \frac{(1-\varsigma\rho)\sin\theta}{(1+\varsigma\rho)\cos\theta + a_2} \tag{8}$$

If we do not take into account the processes of secondary radiation and diffuse reflection from the surface of the sail, then the formulas at Eq. 3, Eq. 4, Eq. 7, Eq. 8 for the thrust from the forces of light pressure and the deviation of the thrust direction from the normal to the surface can be simplified and presented in the following form:

$$a = \frac{S_r}{cm} S(\theta)\sqrt{1 + \rho^2 - 2\rho\cos(\pi - 2\theta)} = \frac{S_r}{cm} S\cos\theta\sqrt{1 + \rho^2 + 2\rho\cos 2\theta}, \tag{9}$$

$$\sin\varphi = \frac{(1-\rho)\sin\theta}{\sqrt{1+\rho^2+2\rho\cos 2\theta}}. \tag{10}$$

Other negative impacts include a narrowing of the range of available acceleration angles relative to the direction of the luminous flux and an increase in the share of absorbed energy of the luminous flux, which leads to an increase in surface temperature and acceleration of degradation processes of the sail surface.

2.3. Degradation of optical parameters of the sail surface

The surface of the sail degrades due to the impact of various factors of outer space. In particular, the reflection coefficient decreases, and the proportion of absorbed radiation increases accordingly. If only solar radiation is taken into account, then the change in optical characteristics can be calculated by the parametric dependencies proposed in [4]:

$$\frac{p(t)}{p_0} = \begin{cases} \frac{1+de^{-\lambda\Sigma(t)}}{1+d} & for\ p \in \{\rho, \varsigma\}, \\ 1 + d\left(1 - e^{-\lambda\Sigma(t)}\right) & for\ p = \varepsilon_f, \\ 1 & for\ \ p \in \{\varepsilon_b, B_f, B_b\}, \end{cases} \tag{11}$$

where $\Sigma(t)$ – the dimensionless total dose of solar radiation received during the flight; λ - degradation coefficient; d - degradation factor. The dimensionless total dose of solar radiation is calculated as the ratio of the total radiation power received by the sail during the flight to the solar radiation power received by a platform of 1 m^2 at a distance of 1 AU in one year $\tilde{\Sigma}_0 = 15{,}768 \cdot 10^{12}$ J/m^2.

$$\Sigma(t) = \frac{\tilde{\Sigma}(t)}{\tilde{\Sigma}_0} = \frac{r_0^2}{T_0}\int_{t_0}^{t} \frac{\cos\theta(t)}{r(t)^2}dt \tag{12}$$

where $T_0 = 365 \cdot 24 \cdot 3600$ s – corresponds to one year in seconds.

The degradation coefficient λ is determined based on half the lifetime of the sail under the influence of solar radiation:

$$\lambda = \frac{\ln 2}{\hat{\Sigma}}. \tag{13}$$

where $\hat{\Sigma}$ - the dose of solar radiation, which leads to a half deterioration of optical characteristics, that is, corresponds to the value of the optical characteristic

$$\hat{p} = \frac{p_0 + p_\infty}{2}.$$

The degradation factor d determines the value of the optical characteristic p_∞, at which the sail should stop functioning. At the same time

$$\rho_\infty = \frac{\rho_0}{1+d}, \qquad \varsigma_\infty = \frac{\varsigma_0}{1+d}, \qquad \varepsilon_{f\infty} = \varepsilon_{f0}(1+d) \tag{14}$$

Even a preliminary analysis of formulas at Eq.11. – 14. shows that the acceleration from the solar sail, and, consequently, the laws of sail control and the corresponding trajectories of motion depend on the optical characteristics of the surface, and the optical characteristics, in turn, depend on the laws of control and flight path. Therefore, a comprehensive analysis of possible interplanetary missions of spacecraft with a solar sail requires taking into account all these interrelated parameters.

3. Solar sail control on the flight sections

3.1. Earth-to-Earth flight and gravity manoeuvre

As we have already mentioned, the entire mission is calculated on the assumption that the trajectory of the spacecraft lies in the plane of the ecliptic and the Earth's orbit is circular. If we consider the passive motion of the spacecraft after leaving the Earth's sphere of action in an orbit with a large semi-axis of 1 AU, then the next meeting of the spacecraft and the Earth will occur in a year. In this case, the variable parameters are the eccentricity of the Earth-to-Earth flight orbit and the radius of the pericentre of the geocentric hyperbola along which the spacecraft will move when performing a gravitational manoeuvre.

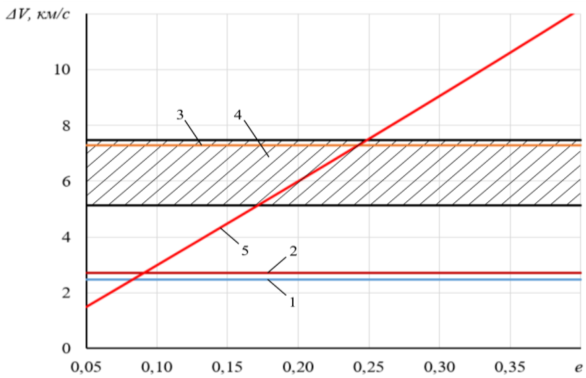

Fig. 4. Graph of the dependence of the required velocity on the eccentricity of the transition orbit. 1 – Venus, 2 – Mars, 3 – Mercury, 4 – Asteroid belt, 5 –the cost of speed to create an Earth-Earth orbit with a given eccentricity

Let's consider the effectiveness of using a gravitational manoeuvre for flights to various objects of the Solar System as in Fig. 4. To do this, compare the costs of the characteristic velocity to reach objects of the Solar System (horizontal lines) and to create a transition orbit with a given eccentricity (inclined line). For example, for a flight to Venus, only with values of eccentricities less than 0.08 – 0.09 we can expend less energy than with a single-pulse manoeuvre. For the flight we are considering to the asteroid belt, the eccentricity of the transition orbit should not be greater than 0.264. Otherwise, it is easier to launch the spacecraft directly into the asteroid belt without using gravitational manoeuvres and a solar sail.

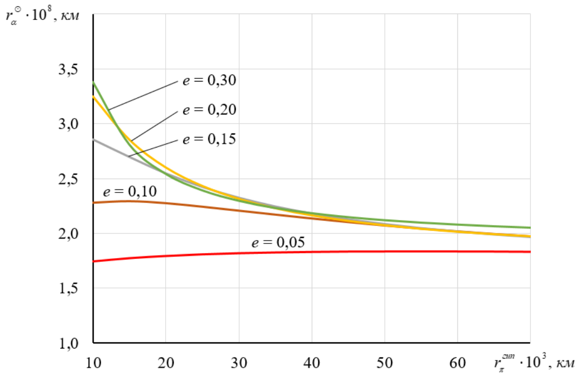

Fig. 5. Graph of the dependence of the aphelion of the resulting orbit on the geocentric perigee and the eccentricity of the transition

Fig.5 shows the aphelion radii of the spacecraft's passive orbits achievable after performing a gravitational manoeuvre. For eccentricities of transition orbits greater than 0.15, the highest aphelion value is achieved at the smallest radii of the pericenter of geocentric orbits. We will use in further calculations a safe distance from the center of the Earth of 10 thousand km and we will get that with the selected eccentricity of the orbit, the maximum value of aphelion 2.27 AU is achieved with the eccentricity of the heliocentric orbit after performing a gravitational manoeuvre 0.41506 and a large semi-axis 1.70958 AU.

During the calculations, we considered the duration of the movement of the section of the geocentric trajectory to change the position and speed of the Earth at the time of completion of the manoeuvre.

3.2. Heliocentric motion control after performing a gravity manoeuvre

In the system of equations of motion Eq. (1), the acceleration from the solar sail ***a*** has two projections, radial a_r and transversal a_u, the direction of which is shown in Fig. 5, and their scalar value can be determined using the acceleration projections calculated by Eq. 3, Eq. 4:

$$a_r = a_\perp \cos\theta + a_{||}|\sin\theta| = a_\perp \cos(\lambda_1 + \varphi) + a_{||}|\sin(\lambda_1 + \varphi)|, \tag{15}$$

$$a_u = a_\perp \sin\theta - a_{||}\cos\theta \cdot sign(\theta) = a_\perp \sin(\lambda_1 + \varphi) - a_{||}\cos(\lambda_1 + \varphi) \cdot sign(\lambda_1 + \varphi) \tag{16}$$

We will look for the law of changing the angle of the sail $\lambda_1 \in \left[-\frac{\pi}{2};\frac{\pi}{2}\right]$, such that it reaches the required orbit as soon as possible, that is, the boundary conditions in Eq. 2 are met and the minimum functionality is provided by

$$T = \int_0^T dt \to \min. \tag{17}$$

To solve this problem, we write down the Hamiltonian:

$$H = P_r \cdot V_r + P_u \cdot \frac{V_u}{r} + P_{V_r}\left(\frac{V_u^2}{r} - \frac{1}{r^2} + \frac{a_c}{r^2}\cos^3\lambda_1\right) + P_{V_u}\left(-\frac{V_u V_r}{r} + \frac{a_c}{r^2}\cos^2\lambda_1 \sin\lambda_1\right)$$

$$\mathrm{H} = V_r\psi_r + \frac{V_u}{r}\psi_u + \left(a_c\frac{\cos^3\theta}{r^2} - - \frac{1}{r^2} + \frac{V_u^2}{r}\right)\psi_{Vr} + \left(a_c\frac{\cos^2\theta\sin\theta}{r^2} - - \frac{V_u V_r}{r}\right)\psi_{Vu}, \tag{18}$$

where P_r, P_u, P_{V_r}, P_{V_u} – conjugate variables, a_c – nominal maximum acceleration acting on the sail at a distance of 1 AU.

According to the Pontryagin maximum principle, the control law and the corresponding trajectory of the device will be optimal if the value of the Hamiltonian is maximal. The control providing the maximum of the Hamiltonian is known [5]:

$$\lambda_1 = \frac{1}{2}\left(\eta - \arcsin\frac{P_{V_u}}{3\sqrt{{P_{V_r}}^2 + {P_{V_u}}^2}}\right), \tag{19}$$

where $\eta = \arccos\frac{P_{V_r}}{\sqrt{{P_{V_r}}^2 + {P_{V_u}}^2}}$.

The next step to determine optimal control is to solve a two-point boundary value problem. The system of equations in Eq. 1 is supplemented by differential equations describing the change of conjugate variables:

$$\begin{aligned}
&\frac{dP_r}{dt} = P_{V_r}\left(\frac{{V_u}^2}{r^2} - \frac{2}{r^3}\right) - P_{V_u}\frac{V_r V_u}{r^2} + \frac{2a_c}{r^3}\cos^3\lambda_1,\\
&\frac{dP_u}{dt} = 0 \Rightarrow \qquad P_u \equiv const,\\
&\frac{dP_{V_r}}{dt} = -P_r + P_{V_u}\frac{V_u}{r},\\
&\frac{dP_{V_u}}{dt} = \frac{P_{V_u}V_r - 2P_{V_r}V_u}{r}.
\end{aligned} \tag{20}$$

If the angular range of the flight is not fixed, then the problem of finding optimal control is reduced to a three-parameter boundary value problem in which it is necessary to find such initial values of conjugate variables that would ensure the fulfillment of boundary conditions in Eq. 2.

3 The results obtained during the simulation

The energy capabilities of the launch vehicle make it possible to launch the spacecraft on a departure trajectory with an eccentricity of the transition orbit of 0.264. The parameters of the passive motion of the spacecraft from the moment of leaving the Earth's sphere of action before performing a gravitational manoeuvre and after it are presented in Table 4.

Table 4 – Parameters of the heliocentric orbit of the spacecraft before the deployment of the solar sail

	Intermediate Earth-Earth orbit	Orbit after gravitational manoeuvre
Big half-axis, million km	149.6	255.75273
Eccentricity	0.264	0.41506
The angle of the true anomaly, deg	105.308	37.233
Radial component of the spacecraft velocity, km/s	7.863	4.802
Transversal component of the spacecraft velocity, km/s	28.728	34.631

After performing the gravitational manoeuvre, the solar sail unfolds, and further movement is carried out with the optimal angle of the sail installation. Fig. 6 - 7 show the optimal change in the angle of installation of the solar sail and the change in the parameters of the flight path after the gravitational manoeuvre.

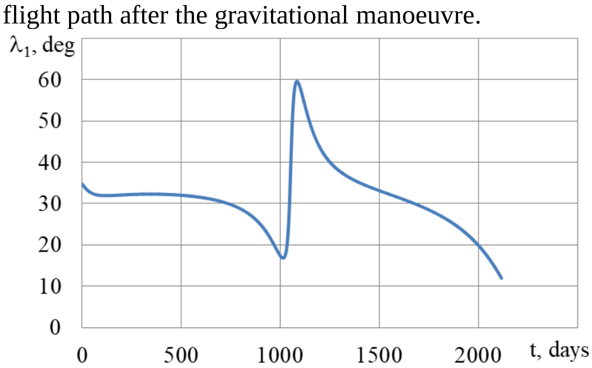

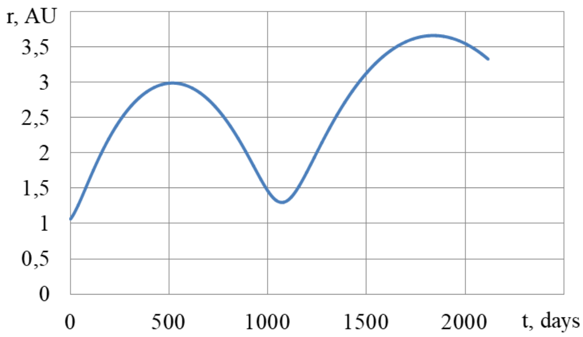

Fig. 6. Changing the angle of the sail and the radius vector of the spacecraft

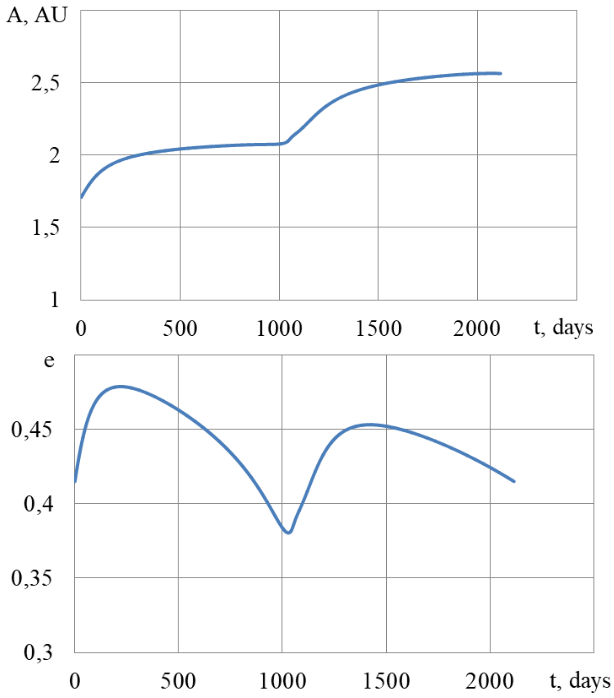

Fig. 7. Change in the semimajor axis and eccentricity of the spacecraft orbit

The duration of the spacecraft's movement to the asteroid belt is 2116.08 days. or about 5.8 years. Considering the passive motion of the spacecraft before the gravitational manoeuvre, the total duration of launching the spacecraft into a working orbit is 6.8 years. Further operation is limited by the service life of scientific devices and power plants.

Fig. 8. shows the full ballistic scheme of the mission, calculated taking into account the degradation of the surface for a sail with an imperfectly reflective surface.

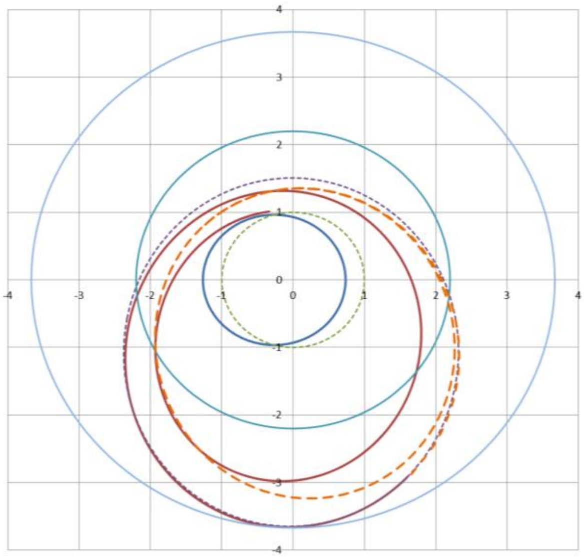

Fig. 8. Full ballistic scheme of spacecraft movement

Fig. 8. shows the trajectory of a spacecraft with a folded sail along an intermediate heliocentric trajectory that provides the specified parameters of a gravitational manoeuvre near the Earth. A year later, after performing a gravitational manoeuvre in the Earth's gravity field, the spacecraft fairing is reset and the solar sail opens. Further heliocentric movement is carried out due to light pressure (dark red fat shedding in Fig. 8). The spacecraft makes a transition to an orbit with an apocenter of 3.6 AU and a pericentre of 1.5 AU, that is, it enters an orbit most of the time lying in the asteroid belt (shown by the purple dotted line). Further changes in the trajectory due to the degradation of the sail are shown by an orange dotted line.

References

[1] Rozhkov, Miroslav A., Olga L. Starinova, and Irina V. Chernyakina, Influence of optical parameters on a solar sail motion, Advances in Space Research 67.9, 2757-2766, 2021

[2] Hughes G.W., Macdonald M., McInnes C.R., и др. Sample return from mercury and other terrestrial planets using solar sail propulsion. Journal of Spacecraft and Rockets. 2006. T. 43, № 4. C. 828–835.

[3] Forward R.L. Grey solar sails. Journal of the Astronautical Sciences. 1989. T. 38, № 2. C. 161–185.

[4] Dachwald B., Macdonald M., McInnes C.R., and others. Impact of optical degradation on solar sail mission performance. Journal of Spacecraft and Rockets. 2007. T. 44, № 4. C. 740–749.

[5] Zhukov A.N., Lebedev V.N. Variational problem of a flight between heliocentric circular orbits using a solar sail. Space Research. 1964, vol. 2, no. 1, pp. 46–50.